horn. Presynaptic neuronal voltage-gated sodium calcium channels are largely responsible for the release of this glutamate as well as the neuropeptide substance P [33]. Microglia also express α-amino-3-hydroxy-5-methyl-4-isoxazolepropionic acid/kainate (AMPA/KA) receptors that mediate the release of inflammatory cytokines such as tumor necrosis factor-α (TNF-α) [34]. AMPA receptors are glutamate receptors that are integral to plasticity and synaptic transmission at many postsynaptic membranes. One of the investigated forms of plasticity in the nervous system is long-term potentiation LTP. LTP explained that glutamate was bound to postsynaptic AMPA receptors. Ligand binding causes AMPA receptors to open and for sodium ions to flow into the postsynaptic cells, resulting in a depolarization. Therefore, we assumed that microglia participated in the changes of glutamatergic synaptic transmission observed at the nerve injury. Receptors expressed on microglial membranes are thought to allow sensing of neuronal activity and/or communication with astrocytes [35]. Glutamate neurotransmission has been associated with pain processing at multiple levels of the neuroaxis [36]. The connections between the C-fibers and the SG neurons play a critical role in pain sensation through an action of the neuropeptides. In the spinal dorsal horn neurons, activation of fine-afferent fibers produce a variety of synaptic events which are likely to be mediated by a number of neurotransmitters, including excitatory amino acids and neuropeptides. We examined the synaptic activities in the superficial dorsal horn neurons response to nerve injury using *in vivo* patch clamp methods. We show EPSC amplitudes were significantly larger following injury distal to the DRG compared with injury proximal to the DRG. In a previous study, EPSC amplitudes obtained from SG neurons at the L5 segmental level of the spinal cord after nerve injury was larger than the sham-operated animals [37]. Interestingly, this is the first study to show significant differences in excitatory synaptic activities in a nerve injury proximal and distal to the DRG. This result also indicates a marked difference in the degree of radiculopathy at distinct points of nerve injuries.

In general, the direction of information flow from the periphery to the DRG to the spinal cord itself is a main factor in the distal lesion giving rise to stronger neuropathic signs. Thus the changes from peripheral inputs are more critical for neuropathy. It has been demonstrated that radiculopathy is caused by changes in the expression and function of receptors and voltage-dependent sodium channels in peripheral nerves and DRG neurons, as well as at synapses in the nociceptive pathway in the CNS [38,39]. In particular, tetrodotoxin resistant (TTX-r) sodium channels are closely related to radiculopathy. The NaV 1.8, which is one of TTX-r sodium channel, is important in the neurophysiological and behavioral effects [40,41]. The NaV 1.8 sodium channels are expressed in both A- and C-fiber populations [42,43] and differentially regulated after peripheral nerve injury, and selectively distributed in peripheral sensory neurons [44]. Sodium channels are involved in the propagation of action potentials, while glutamate receptors expressed on presynaptic terminals of primary afferents in the dorsal horn regulate the release of neurotransmitters. After peripheral nerve injury, injured and uninjured DRG neurons become excitable and exhibit ectopic firing [45,46]. When the spinal nerve is injured distal to the DRG, the DRG neurons become excitable and exhibit ectopic firing, resulting in intense radiculopathy. In this study, there were differences between the degrees of radiculopathy injured proximal or distal to the DRG. This difference of the nerve injury level might have affected the activation and number of sodium channels to which the dorsal root projects. This may have led to activation of glutamatergic transmission, resulting in activation of AMPA receptors and NMDA receptors. As described above, there were differences in the degrees of radiculopathy.

One possible reason for the difference in the degree of radiculopathy at distinct nerve injury points may be due to changes in blood flow. The blood flow in the nerve root is affected by root constriction [47]. The blood flow supply in the nerve root proximal to the DRG is greater compared with blood flow distal to the DRG [48]. Nerve roots are surrounded by cerebrospinal fluid but not the spinal or peripheral nerves. Spinal nerve roots receive 58% of their nutritional supply from cerebrospinal fluid and 38% from intramural blood vessels, whereas peripheral nerves receive 95% of their nutritional supply from intramural blood vessels [49]. Another possible reason for the difference in the degree of radiculopathy may be the number of apoptotic neurons in the spinal cord. Expression of apoptosis in the spinal cord was found to be associated with radiculopathy after spinal nerve or nerve root injuries [50]. The percentage of apoptosis in the DRG was significantly increased in the distal crush group compared with the proximal crush group. This difference in response was because the DRG was not injured directly, resulting in apoptosis secondary to the nerve injuries [51].

Conclusion

We investigated the degree of radiculopathy using different points of mechanical sensitivity, immunohistochemistry and *in vivo* patch-clamp recordings. Our study indicated that there was a more intense radiculopathy following injury distal to the DRG rather than proximal to the DRG. Indicating the degree of radiculopathy is dependent on the level of nerve injury.

Materials and methods

A total of 125 adult male Sprague–Dawley rats weighing 180–210 g were used in this study. Animals were housed in plastic cages at room temperature on a 12-h light/dark

cycle with free access to food and water. All animal experimental procedures were approved by the Ethics Committee on Animal Experiments, Wakayama Medical University and were performed in accordance with the UK Animals (Scientific Procedures) Act of 1986 and associated guidelines.

Surgical protocol for the radiculopathy model

The surgical protocol was modified from the lumbar radiculopathy model, as previously reported [52-54]. Rats were divided into five groups at random: Normal (group A), sham (group B), ligated proximal to the DRG (group C), ligated at the DRG (group D), ligated distal to the DRG (group E). The rats were anesthetized with sodium pentobarbital (50 mg/kg, i.p.), placed into a prone position, and received an incision to the middle of the spine at the L4-L6 level. The paraspinal muscles were retracted to expose the right laminas and facet joints between the L4 and L6 vertebrae. A right L5 hemilaminectomy and foraminotomy was performed. The right L5 nerve and DRG were carefully exposed not to influence the electrical properties. The injury was created by ligating the nerve root 2 mm proximal to the DRG (group C), at the DRG (group D) and at the spinal nerve 2 mm distal to the DRG (group E) using 6.0 silk sutures. [Figure 1A] Great care was taken to ligate such that the diameter of the nerve was seen to be just ligated by a microscope at 5× magnification. The desired degree of constriction retarded, but did not arrest, circulation through the superficial epineural vasculature and sometimes produced a small, brief twitch in the muscle surrounding the exposure [54]. After enough washing, the incision was closed in layers. Rats were allowed to recover in their normal environment. Two groups of control rats were used; One was not operated on (group A), the other received sham procedures, a right L5 nerve root exposure without ligation (group B).

Mechanical sensitivity

The hind paw withdrawal threshold was measured as the frequency of foot withdrawals elicited by a defined mechanical stimulus using a 10 g von Frey filament [55,56]. The rats were placed in a chamber, measuring 18 × 25 × 18 cm above a wire mesh floor. They were acclimatized to the environment and investigator for at least 20 minutes before the test. A evaluation was performed approximately 7 days (7.8 ± 2.1 days, 220.5 ± 21.6 g, n = 50) after surgery.

The mechanical stimulus was applied to the middle area between the footpads on the plantar surface of the ipsilateral (nerve root injury site) hind paw and maintained for approximately 2 seconds. A withdrawal response was considered valid only if the hind paw was removed completely from the platform. If a rat walked immediately after stimulation of a hair instead of lifting the paw, the hair was reapplied. A trial consisted of application of a von Frey hair to the hind paw five times at 5-second intervals. The hind paw was probed consecutively with 10 stimulations. The trial was repeated 3 times with at least a 10-minute interval. Mechanical sensitivity was evaluated as the frequency of withdrawal responses, expressed as the mean frequency of responses.

Differences between groups were compared using Student's t test or a one-way analysis of variance (ANOVA). Data were presented as mean ± SEM. When ANOVA showed a significant difference, pair-wise comparisons between means were tested by the *post-hoc* Tukey method. Hind paw withdrawal threshold values between groups were considered significantly different with a P value < 0.05.

Immunohistochemistry

Spinal sections were processed for immunohistochemistry using the immunofluorescence [57,58].

At 7 days post-surgery, rats (208.4 ± 21.7 g, n = 25) were perfused through the ascending aorta with saline followed by 4% paraformaldehyde with 1.5% picric acid in 0.16 M phosphate buffer, pH7.2–7.4 (4°C). After perfusion, spinal cords were removed and the L4-L5 spinal cord segments were dissected, post fixed in the same perfusion fixative for 4 hours and then 15% sucrose overnight. All of the spinal cords for each experiment were arranged on the same blocks with optimal cutting temperature embedding medium and mounted on the same slides after sectioning. Transverse spinal sections (15 μm) were cut on a cryostat and processed for immunostaining. Spinal sections were blocked with 2% goat serum in 0.3% Triton X-100 for 1 hour at room temperature and incubated overnight at 4°C with rabbit (polyclonal) antiserum directed against the ionized calcium binding adapter molecule 1 (Iba1; 1:1000; Wako Chemicals, Tokyo, Japan), a marker of microglia [59].

After washing, the sections were then incubated with fluorescent–conjugated secondary antibody (1:1000 Alexa Fluor 594 goat anti-rabbit; Invitrogen, San Diego, CA) for 90 minutes at room temperature.

The immunostained sections were examined and photographed with an Olympus (FSX100, Japan) fluorescence microscope at 40× magnification. Quantification of microglia activation was assessed by the number of Iba1-positive microglia in the lamina I–II of the L5 segment.

Differences between groups were compared using Student's t test or a one-way ANOVA. Data were presented as mean ± SEM. When ANOVA showed a significant difference, pair-wise comparisons between means were tested by the *post-hoc* Tukey method. Values were considered statistically significant with a P value < 0.05.

In vivo patch-clamp recordings

The methods used for the *in vivo* patch-clamp recordings were as described previously [6,7,60,61]. Rats (218.4 ± 23.5 g, n = 45) were assessed approximately 7 days (7.6 ± 2.4 days) post- surgery when mechanical hypersensitivity had developed fully. Rats were anesthetized with urethane (1.2 g/kg, i.p.). Artificial ventilation of the pneumothorax was not performed as the rats could be maintained in good condition by supplying oxygen through a nose cone [60]. If a withdrawal reflex appeared, a supplemental dose of urethane was given during surgery and the data collection period. A heating pad was placed beneath the rat to maintain its body temperature at 37–38°C. The rat was placed in a stereotaxic apparatus (Model STS-B&SR-5R-HT, Narishige, Tokyo, Japan) and lumbar spinal cord at the L5 segmental area was exposed by a thoracolumbar laminectomy at the level from Th12 to L2. The dura was cut under a microscope with 40× magnification and a recording electrode was advanced into the SG from the surface of the spinal cord. The pia-arachnoid membrane of the right L5 dorsal root entry zone was removed allowing the patch electrode to enter the spinal cord. The surface of the spinal cord was irrigated with Krebs solution (10–15 ml/min) and equilibrated with a 95% O_2, 5% CO_2 gas mixture (117 mM NaCl, 3.6 mM KCl, 2.5 mM $CaCl_2$, 1.2 mM $MgCl_2$, 1.2 mM NaH_2PO_4, 11 mM glucose and 25 mM $NaHCO_3$) through glass pipettes at 36.5 ± 0.5°C. At the end of the experiments, the rats were given an overdose of urethane and killed by exsanguinations.

The patch electrodes were pulled from thin-walled borosilicate glass capillaries (outer diameter of 1.5 mm, TW150F-4, World Precision Instruments, Sarasota, FL, USA) using a p-97 puller (Sutter Instrument, Novato, CA, USA) and filled with a patch-pipette solution that contained: 135 mM K-gluconate, 5 mM KCl, 0.5 mM $CaCl_2$, 2 mM $MgCl_2$, 5 mM EGTA, 5 mM ATP-Mg and 5 mM Hepes-KOH; pH7.2 for excitatory postsynaptic current (EPSC) recordings. The recording electrode with a resistance of 8-12MΩwas advanced at an angle of 30 degrees into the SG through the pia-arachnoid membrane by a micromanipulator (Model MWS-32 S, Narishige, Tokyo, Japan). A gigaohm seal (resistance of 10GΩ) was formed with neurons at a depth of 30–150 μm from the surface of the spinal cord, the membrane patch ruptured because of a period of negative pressure and the whole-cell patch-clamp recording was initiated. Holding potential was set to −70 mV in voltage-clamp mode and recordings were collected using an Axopatch 200B amplifier in conjunction with a Digidata 1440A A/D converter (Molecular Devices, Sunnyvale, CA, USA) and stored on a computer using pCLAMP 10 data acquisition program (Molecular Devices, Sunnyvale, CA, USA).

Differences between groups were compared using Student's *t* test or a one-way ANOVA. Data were presented as mean ± SEM. When ANOVA showed a significant difference, pair-wise comparisons between means were tested by the *post-hoc* Tukey method. Values were considered statistically significant with a P value < 0.05.

Abbreviations

DRG: Dorsal root ganglia; SG: The substantia gelatinosa; LTP: Long term potential; CNS: Central nervous system; EPSC: Excitatory postsynaptic currents; IPSC: Inhibitory postsynaptic currents; NMDA receptor: N-methyl D-aspartate receptor; AMPA receptor: α-amino-3-hydroxy-5-methyl-4-isoxazole propionic acid receptor; Iba 1: Anti-ionized calcium binding adapter molecule 1; TTX-r sodium channel: Tetrodotoxin resistant sodium channel.

Competing interests

The authors declare that they have no competing interests.

Acknowledgements

This work was supported in part by MEXT KAKENHI 23592174 to HH and MEXT KAKENHI 23592173 to MY and MEXT KAKENHI 2279139 to WT and MEXT KAKENHI 22591647 to TN There are no conflicts of interest regarding this study, for any of the authors.

Author details

[1]Department of Orthopaedic Surgery, Wakayama Medical University, 811-1 Kimiidera, Wakayama 641-8509, Japan. [2]Pain Research Center, Kansai University of Health Sciences, 2-11-1 Wakaba Kumatori Sennan, Osaka 590-0482, Japan.

Authors' contributions

All authors read and approved the final manuscript. NT performed or contributed to all experiments, analyzed data and drafted the paper. WT and HH contributed to experiments and analysis. NN contributed to experiments. NM and HY participated in the design of the studies. TN and MY conceived and supervised the project and edited the manuscript.

Received: 23 February 2012 Accepted: 6 April 2012
Published: 26 April 2012

References

1. Willis WD, Coggeshall RE: *Sensory mechanisms of the spinal cord*. New York, NY: Plenum; 1991:153–215.
2. Schneider SP, Perl ER: **Comparison of primary afferent and glutamate excitation of neurons in the mammalian spinal dorsal horn.** *J Neurosci* 1988, **8**:2062–2073.
3. Nakatsuka T, Ataka T, Kumamoto E, Tamaki T, Yoshimura M: **Alteration in synaptic inputs through C-afferent fibers to substantia gelatinosa neurons of the rat spinal dorsal horn during postnatal development.** *Neuroscience* 2000, **99**:549–556.
4. Mendell LM, Wall PD: **Responses of single dorsal cord cells to peripheral cutaneous unmyelinated fibres.** *Nature* 1965, **206**:97–99.
5. Randic M, Jiang MC, Cerne R: **Long-term potentiation and long-term depression of primary afferent neurotransmission in the rat spinal cord.** *J Neurosci* 1993, **13**:5228–5241.
6. Furue H, Narikawa K, Kumamoto E, Yoshimura M: **Responsiveness of rat substantia gelatinosa neurons to mechanical but not thermal stimuli revealed by in vivo patch-clamp recording.** *J Physiol* 1999, **521**:529–535.
7. Narikawa K, Furue H, Kumamoto E, Yoshimura M: **In vivo patch-clamp analysis of IPSCs evoked in rat substantia gelatinosa neurons by cutaneous mechanical stimulation.** *J Neurophysiol* 2000, **84**:2171–2174.
8. Watkins LR, Milligan ED, Maier SF: **Glial activation: a driving force for pathological pain.** *Trends Neurosci* 2001, **24**:450–455.
9. Tsuda M, Inoue K, Salter MW: **Neuropathic pain and spinal microglia: a big problem from molecules in "small" glia.** *Trends Neurosci* 2005, **28**:101–107.
10. Inoue K, Tsuda M: **Microglia and neuropathic pain.** *Glia* 2009, **57**:1469–1479.
11. Colburn RW, Richman AJ, DeLeo JA: **The effect of site and type of nerve injury on spinal glial activation and neuropathic pain behavior.** *Exp Neurol* 1999, **157**:289–304.

12. Raivich G, Bohatschek M, Kloss C, Werner A, Jones LL, Kreutzberg GW: **Neuroglial activation repertoire in the injured brain: graded response, molecular mechanisms and cues to physiological function.** *Brain Res Rev* 1999, **30**:77–105.
13. Tsuda M, Shigemoto-Mogami Y, Koizumi S, Mizokoshi A, Kohsaka S, Salter MW, Inoue K: **P2X4 receptors induced in spinal microglia gate tactile allodynia after nerve injury.** *Nature* 2003, **424**:778–783.
14. Beggs S, Salter MW: **Stereological and somatotopic analysis of the spinal microglial response to peripheral nerve injury.** *Brain Behav Immun* 2007, **21**:624–633.
15. Clark AK, Yip PK, Grist J, Gentry C, Staniland AA, Marchand F, Dehvari M, Wotherspoon G, Winter J, Ullah J, Bevan S, Malcangio M: **Inhibition of spinal microglial cathepsin S for the reversal of neuropathic pain.** *Proc Natl Acad Sci USA* 2007, **104**:10655–10660.
16. Zhang J, Shi XQ, Echeverry S, Mogil JS, De Koninck Y, Rivest S: **Expression of CCR2 in both resident and bone marrow-derived microglia plays a critical role in neuropathic pain.** *J Neurosci* 2007, **27**:12396–12406.
17. Thacker MA, Clark AK, Bishop T, Grist J, Yip PK, Moon LD, Thompson SW, Marchand F, McMahon SB: **CCL2 is a key mediator of microglia activation in neuropathic pain states.** *Eur J Pain* 2009, **13(3)**:263–272.
18. Abdullah AF, Ditto EW, Byrd EB, Williams R: **Extreme-lateral lumbar disc herniations: clinical syndrome and special problems of diagnosis.** *J Neurosurg* 1974, **41**:229–234.
19. Siebner HR, Faulhauer K: **Frequency and specific management of far lateral lumbar disc herniations.** *Acta Neurochir (Vienna)* 1990, **105**:124–131.
20. Novetsky GJ, Berlin L, Epstein AJ, Lobo N, Miller SH: **The extraforaminal herniated disk: detection by computed tomography.** *AJNR* 1982, **3**: 653–655.
21. Ito T, Ohtori S, Inoue G, Koshi T, Doya H, Ozawa T, Saito T, Moriya H, Takahashi K: **Glial phosphorylated p38 MAP kinase mediated pain in a rat model of lumbar disc herniation and induces motor dysfunction in a rat model of lumbar spinal canal stenosis.** *Spine* 2007, **32**:159–167.
22. Sekiguchi Y, Kikuchi S, Myers RR, Campana WM: **Erythropoietin inhibits spinal neuronal apoptosis and pain following nerve root crush.** *Spine* 2003, **28**:2577–2584.
23. Chatani K, Kawakami M, Weinstein JN, Meller ST, Gebhart GF: **Characterization of thermal hyperalgesia, c-fos expression, and alterations in neuropeptides after mechanical irritation of the dorsal root ganglion.** *Spine (Phila Pa 1976)* 1995, **20**:277–289.
24. Kim SH, Chung JM: **An experimental model for peripheral neuropathy produced by segmental spinal nerve ligation in the rat.** *Pain* 1993, **50**:355–363.
25. Svensson CI, Hua XY, Protter AA, Powell HC, Yaksh TL: **Spinal p38 MAP kinase is necessary for NMDA-induced spinal PGE(2) release and thermal hyperalgesia.** *Neuroreport* 2003, **14**:1153–1157.
26. Ji RR, Kohno T, Moore KA, Woolf CJ: **Central sensitization and LTP: do pain and memory share similar mechanisms?** *Trends Neurosci* 2003, **26**:696–705.
27. Hu B, Chiang CY, Hu JW, Dostrovsky JO, Sessle BJ: **P2X receptors in trigeminal subnucleus caudalis modulate central sensitization in subnucleus caudalis oralis.** *J Neurophysiol* 2002, **88**:1614–1624.
28. Afrah AW, Fiska A, Gjerstad J, Gustafsson H, Tjolsen A, Olgart L, Stiller CO, Hole K, Brodin E: **Spinal substance P release in vivo during the induction of long-term potentiation in dorsal horn neurons.** *Pain* 2002, **96**:49–55.
29. Sluka KA, Westlund KN: **Spinal cord amino acid release and content in an arthritis model: the effects of pretreatment with non-NMDA, NMDA, and NK1 receptor antagonists.** *Brain Res* 1993, **627**:89–103.
30. Parpura V, Basarsky TA, Liu F, Jeftinja S, Haydon PG: **Glutamate-mediated astrocyte-neuron signaling.** *Nature* 1994, **369**:744–747.
31. Schell MJ, Molliver ME, Snyder SH: **D-Serine, an endogenous synaptic modulator: localization to astrocytes and glutamate-stimulated release.** *Proc Natl Acad Sci U S A* 1995, **92**:3948–3952.
32. Schipke C, Ohlemeyer C, Matyash M, Nolte N, Kirchhoff F: **Astrocytes of mouse neocortex express functional N-Methyl D-Aspartate (NMDA) receptors.** *FASEB J* 2001, **15**:1270–1272.
33. Baron R: **Mechanisms of disease: neuropathic pain-a clinical perspective.** *Nat Clin Pract Neurol* 2006, **2**:95–106.
34. Noda M, Nakanishi H, Nabekura J, Akaike N: **AMPA-preferring subtypes of glutamate transporter is enhanced by amyloid-βpeptide.** *Neurosci* 1999, **92**:1465–1474.
35. Pocock JM, Kettenmann H: **Neurotransmitter receptors on microglia.** *Trends Neurosci* 2007, **30**:527–535.
36. Corderre TJ: **The role of excitatory amino acid receptors and intracellular messengers in persistent nociception after tissue injury in rats.** *Mol Neurobiol* 1994, **7**:229–246.
37. Terashima Y, Kawamata M, Takebayashi T, Tanaka S, Tanimoto K, Yamashita T: **Changes in synaptic transmission of substantia gelatinosa neurons in a rat model of lumbar radicular pain revealed by in vivo patch-clamp recording.** *Pain* 2011, **152**(5):1024–1032.
38. Scholz J, Woolf CJ: **The neuropathic pain triad: neurons, immune cells and glia.** *Nat Neurosci* 2007, **10**:1361–1368.
39. Reichling DB, Levine JD: **Critical role of nociceptor plasticity in chronic pain.** *Trends Neurosci* 2009, **32**:611–618.
40. Dong XW, Goregoaker S, Engler H, Zhou X, Mark L, Crona J, Terry R, Hunter J, Priestley T: **Small interfering RNA-mediated selective knockdown of NaV 1.8 tetrodotoxin-resistant sodium channel reverses mechanical allodynia in neuropathic rats.** *Neuroscience* 2007, **146**:812–821.
41. Lai J, Gold MS, Kim CS, Bian D, Ossipov MH, Hunter JC, Porreca F: **Inhibition of neuropathic pain by decreased expression of the tetrodotoxin-resistant sodium channel, NaV 1.8.** *Pain* 2002, **95**:143–152.
42. Djouhri L, Fang X, Okuse K, Wood JN, Berry CM, Lawson SN: **The TTX-resistant sodium channel Nav 1.8 (SNS/PN3): expression and correlation with membrane properties in rat nociceptive primary afferent neurons.** *J Physiol* 2003, **550**:739–752.
43. Novakovic SD, Tzoumaka E, McGivern JG, Haraguchi M, Sangameswaran L, Gogas KR, Eglen RM, Hunter JC: **Distribution of the tetrodotoxin-resistant sodium channel PN3 in the rat sensory neurons in normal and neuropathic conditions.** *J Neurosci* 1998, **18**:2174–2187.
44. Wood JN, Boorman JP, Okuse K, Baker MD: **Voltage-gated sodium channels and pain pathways.** *J Neurobiol* 2004, **61**:55–71.
45. Devor M: **Ectopic discharge in Abeta afferents as a source of neuropathic pain.** *Exp Brain Res* 2009, **196**:115–128.
46. Wu G, Ringkamp M, Hartke TV, Murinson BB, Campbell JN, Griffin JW, Meyer RA: **Early onset of spontaneous activity in uninjured C-fiber nociceptors after injury to neighboring nerve fibers.** *J Neurosci* 2001, **21**:RC140.
47. Olmarker K, Holm S, Rydevik B: **Experimental nerve root compression. A model of acute, graded compression of the porcine cauda equine and an analysis of neural and vascular anatomy.** *Spine* 1991, **16**:61–69.
48. Naito M, Owen JH, Bridwell K, Oakley D: **Blood flow direction in the lumbar nerve root.** *Spine* 1990, **15**:966–968.
49. Rydevik B, Holm S, Brown MD, Lundborg G: **Diffusion from the cerebrospinal fluid as a nutritional pathway for spinal nerve roots.** *Acta Physiol Scand* 1990, **138**:247–248.
50. Hatashima S, Sekiguchi M, Kobayashi H, Konno S, Kikuchi S: **Contralateral neuropathic pain and neuropathology in dorsal root ganglion and spinal cord following hemilateral nerve injury in rats.** *Spine* 2008, **33**:1344–1351.
51. Sekiguchi M, Sekiguchi Y, Konno S, Kobayashi H, Homma Y, Kikuchi S: **Comparison of neuropathic pain and neuronal apoptosis following nerve root or spinal nerve compression.** *Eur Spin J* 2009, **18**:1978–1985.
52. Kawakami M, Weinstein JN, Spratt KF, Chatani K, Traub RJ, Meller ST, Gebhart GF: **Experimental lumbar radiculopathy. Immunohistochemical and quantitative demonstrations of pain induced by lumbar nerve root irritation of the rat.** *Spine (Phila Pa 1976)* 1994, **19**:1780–1794.
53. Kirita T, Takebayashi T, Mizuno S, Takeuchi H, Kobayashi T, Fukao M, Yamashita T, Torse N: **Electrophysiologic changes in dorsal root ganglion neurons and behavioral changes in a lumbar radiculopathy model.** *Spine (Phila Pa 1976)* 2007, **32**:E65-E72.
54. Bennet GJ, Xie YK: **A peripheral mononeuropathy in rat that produces disorders of pain sensation like those seen in man.** *Pain* 1988, **33**:87–107.
55. Colburn RW, DeLeo JA, Richman AJ, Yeager MP, Kwon P, Hickey WF: **Dissociation of microglial activation and neuropathic pain behavior following peripheral nerve injury in the rat.** *J Neuroimmunol* 1997, **79**: 163–175.
56. Pitcher GM, Ritchie J, Henry JL: **Paw withdrawal threshold in the von Frey hair test is influenced by the surface on which the rat stands.** *J Neurosci Methods* 1999, **87**:185–193.
57. Ji RR, Zhang X, Wiesenfeld-Hallinz Z, Hokfelt T: **Expression of neuropeptide Y and neuropeptide Y (Y1) receptor m RNA in rat spinal cord and dorsal root ganglia following peripheral tissue inflammation.** *J Neurosci* 1994, **14**:6423–6434.
58. Kawasaki Y, Kohno T, Zhuang ZY, Brenner GJ, Wang H, Van Der Meer C, Befort K, Woolf CJ, Ji RR: **Ionotropic and Metabotropic Receptors, Protein Kinase A, Protein Kinase C, and Src contribute to C-Fiber-induced ERK**

activation and cAMP response element-binding protein phosphorylation in dorsal horn neurons, leading to central sensitization. *J Neurosci* 2004, 24:8310–8321.
59. Imai Y, Ibata I, Ito D: **A novel gene iba1 in the major histocompatibility complex class III region encoding an EF hand protein expressed in a monocytic lineage.** *Biophys Biochem Res Commun* 1996, **224**:855–862.
60. Sonohata M, Furue H, Katafuchi T, Yasaka T, Doi A, Kumamoto E, Yoshimura M: **Actions of noradrenaline on substantia gelatinosa neurons in the rat spinal cord revealed *in vivo* patch-clamp recording.** *J Physiol* 2003, 555:515–526.
61. Taniguchi W, Nakatsuka T, Miyazaki N, Yamada H, Takeda D, Fujita T, Kumamoto E, Yoshida M: ***In vivo* patch-clamp analysis of dopaminergic antinociceptive actions on substantia gelatinosa neurons in the spinal cord.** *Pain* 2011, 152:95–105.

doi:10.1186/1744-8069-8-31
Cite this article as: Takiguchi *et al.*: Distinct degree of radiculopathy at different levels of peripheral nerve injury. *Molecular Pain* 2012 8:31.

Efficacy of Novel Minimally Invasive Surgery Using Spinal Microendoscope For Treating Extraforaminal Stenosis at the Lumbosacral Junction

Hiroshi Yamada, MD, PhD, Munehito Yoshida, MD, PhD, Hiroshi Hashizume, MD, PhD, Akihito Minamide, MD, PhD, Yukihiro Nakagawa, MD, PhD, Masaki Kawai, MD, Hiroshi Iwasaki, MD, PhD, and Syunji Tsutsui, MD, PhD

Study Design: A retrospective case study of the spinal microendoscopic surgery for the treatment of extraforaminal stenosis at the lumbosacral junction.

Objective: To evaluate the efficacy of a minimally invasive technique using spinal microendoscope and to examine the 2-year surgical outcome for this disease.

Summary of Background Data: The paraspinal approach has been the gold standard to expose the extraforaminal space. Although it seems to be ideal, the constricted surgical field of view may compromise the surgeon's ability and increase the risk of complications. This technique can be improved further.

Methods: A total of 32 patients, who completed a minimum follow-up of 2 years after the surgery, were included in this study. The study group consisted of 16 men and 16 women with an average age at surgery of 64 years and a mean follow-up of 37.4 months. Clinical results were evaluated according to the Japanese Orthopaedic Association (JOA) scoring system, visual analog scale, and the North American Spine Society Low Back Outcome Instrument.

Results: Two of these patients required revision surgery to correct insufficient decompression in the foramen. In the 30 other patients, the mean JOA score was 15.1 points before surgery and 23.1 points at the final follow-up. The mean recovery rate was 60.1%. The JOA scores improved significantly after surgery and the satisfactory results were maintained until the final follow-up. The visual analog scale scores for low-back pain, leg pain, and numbness also significantly improved. Twenty-eight of 32 patients (87.6%) were satisfied with this procedure.

Conclusions: The spinal microendoscopic surgery demonstrated efficacy for treating extraforaminal stenosis at the lumbosacral junction where the lesion is difficult to be exposed. Quick and easy access along with minimal damage to the back muscles and bony structures could be accomplished using the property of its oblique view and angled surgical equipments. This procedure has produced long-lasting favorable outcomes and high patient satisfaction. Novel minimally invasive surgery may replace conventional open methods.

Key Words: lumbar spine, extraforaminal stenosis, spinal microendoscopy

(*J Spinal Disord Tech* 2012;25:268–276)

Extraforaminal stenosis at the lumbosacral junction, including the famous "far-out syndrome,"[1] is a rare disease pattern,[2–8] although the number of surgical cases has increased in recent years.[9,10] It is suggested that the advent of 3-dimensional imaging diagnostic technology has improved the ability to diagnose such lesions[11] in an area previously called the "hidden zone"[12] and has led to an increase in disease prevalence rate.

Surgical techniques to treat extraforaminal stenosis at the lumbosacral junction have been regarded as a difficult challenge. In the conventional midline approach, the back muscle mass and the prominence of the posterior iliac crest often make it difficult to expose the operative field, which is much deeper than that in ordinary posterior spinal surgery. Bleeding from a rich blood vessel supply also presents problems for coagulating within this deep and narrow working space. The paraspinal muscle-splitting approach first reported by Wiltse and Spencer[13] was considered revolutionary when introduced because it allowed the surgeon to reach the deep site from the body surface without cutting many of the supporting structures. Therefore, the paraspinal approach has been the gold standard for obtaining adequate exposure of the extraforaminal zone at the lumbosacral junction.

Although the paraspinal approach seems to be ideal, the authors believe that this technique can be improved further. For example, the incision must be expanded more than may be necessary and special surgical equipments such as headlight, magnifiers, and special retractors are needed because of the deep location in the body. The

Received for publication October 24, 2010; accepted April 12, 2011.
From the Department of Orthopedic Surgery, Wakayama Medical University, Wakayama, Japan.
The authors declare no conflict of interest.
Reprints: Hiroshi Yamada, MD, PhD, Department of Orthopedic Surgery, Wakayama Medical University, 811-1 Kimiidera, Wakayama, Wakayama 641-8510, Japan (e-mail: yamacha@wakayama-med.ac.jp).

constricted surgical field of view may compromise the surgeon's ability and increase the risk of complications.

By contrast, the greatest benefit of spinal microendoscopy is that the apparatus can reach a deep site expeditiously and can provide a bright, magnified visual surgical field without any retraction of the paravertebral muscles.[14] This allows the surgeon to avoid unnecessary invasion of the surrounding tissues other than the nerve decompression procedure. This novel surgical technique may replace conventional open methods and may improve the surgical outcome for extraforaminal stenosis at the lumbosacral junction.

The aim of this study was to assess the feasibility and efficacy of a minimally invasive technique using spinal microendoscope and to examine the 2-year surgical outcome in patients with extraforaminal stenosis at the lumbosacral junction.

MATERIALS

Since 2005, a clinical trial of microendoscopic extraforaminal decompression has been conducted at our institute. All patients with fifth lumbar radiculopathy caused by extraforaminal stenosis at the lumbosacral junction were consecutively enrolled. The inclusion criteria were medically intractable lumbar spinal stenosis with or without degenerative scoliosis. Patients with dynamic segmental instability such as degenerative spondylolisthesis greater than grade II and isthmic spondylolisthesis were excluded. Moreover, there is one more factor that is important for exclusion criteria in this study. That is a case of double lesions of fifth lumbar spinal nerve. There are many cases with the lesions existing in both intracanal at L4-5 and extraforaminal zone at the lumbosacral junction along the nerve pathways on the preoperative imaging studies. To describe the surgical results of extraforaminal decompression at the lumbosacral junction, the patients with true-positive double lesions confirmed by intraoperative findings were excluded. In this cohort, 32 patients (16 men and 16 women) with a minimum follow-up duration of 2 years postoperatively were included in this study.

Diagnosis

Extraforaminal stenosis was defined as a disease state where the stenotic lesion exists mainly outside the outer border of the intervertebral foramen.[4] Diagnosing this lesion is difficult using conventional imaging studies such as plain x-rays, computed tomography (CT), myelograms, and CT myelograms. Parasagittal magnetic resonance (MR) images are the gold standard for exploring abnormalities around the foramen. The most suggestive finding is a decrease in or disappearance of perineural fat tissue surrounding the nerve root.[15] Although this finding may be effective for diagnosing foraminal stenosis, MR images do not give complete information and sometimes produce false-negative findings of extraforaminal stenosis existing outside the intervertebral foramen (Figs. 1A, B). Therefore, the presence of extraforaminal stenosis may be overlooked and the failure to recognize these lesions may have led to unsatisfactory surgical results.

To avoid misdiagnosis or missing the lesion, the authors relied on routine 3-dimensional-MR imaging studies before surgery. This modality can visualize directly the nerve element outside the foramen.[11] All the patients in

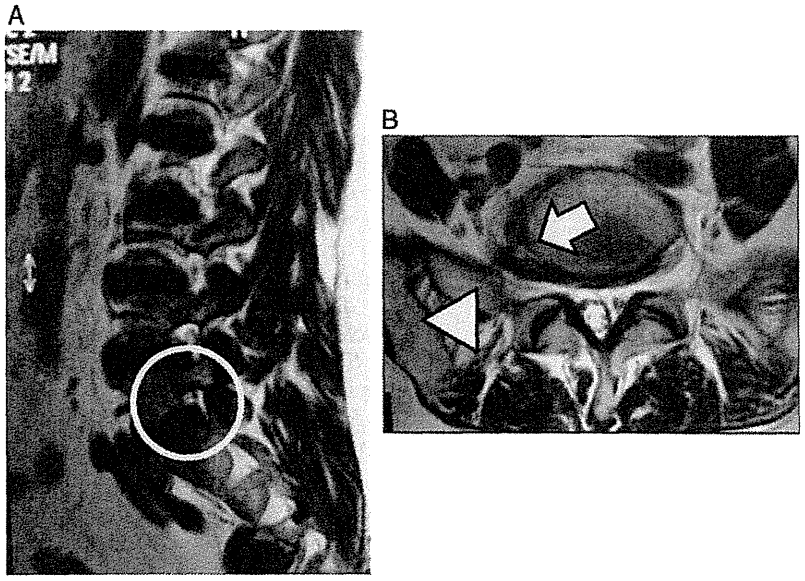

FIGURE 1. An example of conventional magnetic resonance images in case of extraforaminal stenosis at the lumbosacral junction. A, On the T2-weighted parasagittal view of right L5-S1 foramen, no obvious stenotic lesion is observed (open white circle). B, On the axial view at the level of L5-S1 segment, although the existence of bony stenosis between the posterolaterally developed bony spur of L5 vertebral body (white arrow) and the sacral ala (white triangle) is suspected on the right, it is difficult to determine whether there is nerve compression.

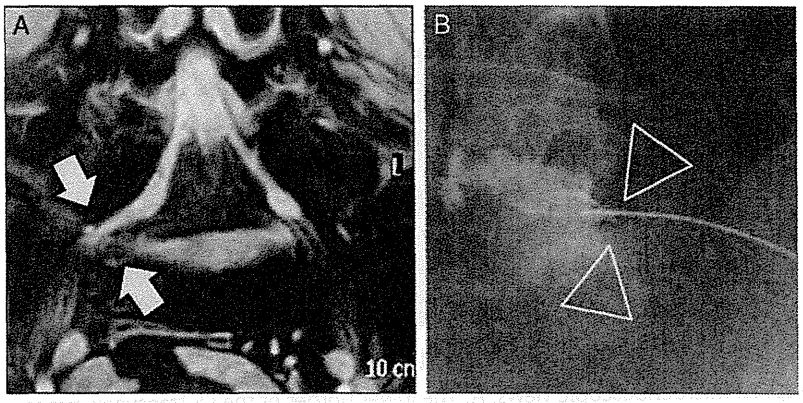

FIGURE 2. An example of 3-dimensional imaging study and selective radiculography of fifth lumbar spinal nerve in case of extraforaminal stenosis at the lumbosacral junction. A, On the multiplanar reformat view obtained from 3-dimensional-magnetic resonance imaging studies, extraforaminal entrapment of the fifth lumbar spinal nerve between the bony spur and the sacral ala is clearly demonstrated (white arrows). The swelling of the nerve and spinal ganglion is also well depicted. B, Selective radiculography of the fifth lumbar spinal nerve shows complete block in the extraforaminal zone (open white triangles), which usually occurs between the sacral ala and osteophyte projecting laterally off the inferior endplate of the L5 vertebra.

this series showed spinal nerve constriction at the extraforaminal zone in a multiplanar reformat coronal view obtained using 3-dimensional-MR imaging studies (Fig. 2A). Nerve root swelling was frequently concomitant with this finding. These findings strongly suggest that extraforaminal entrapment of the fifth lumbar spinal nerve causes the radicular symptoms. In addition, subsequently selective radiculography of the fifth lumbar spinal nerve demonstrated partial or complete block in the extraforaminal zone. This usually occurred between the sacral ala and osteophyte that projected laterally off the inferior endplate of the L5 vertebra (Fig. 2B). The final diagnosis was established when radicular symptoms and neurogenic intermittent claudication were relieved temporarily or disappeared after L5 nerve root blocking.

Operative Technique

Nerve decompression was performed by posterior spinal microendoscopic surgery using the METRx MED system (Medtronic Sofamor Danek). Patients were operated on under general anesthesia. After intubation, the patient was placed in the prone position on a 4-poster spinal frame. Under fluoroscopic guidance, the transverse process, lateral aspect of the L5-S1 facet, and sacral ala (TLS triangle) were drawn on the skin surface. A skin incision with 16 mm sides was made in the shape of triangle formed by the 3 bony structures' configurations (TLS triangle) and a tubular retractor was introduced into the extraforaminal zone (Figs. 3A, B). After clear demonstration of the posterior surface of these bony structures, the lumbosacral ligament was first identified as a landmark for bony decompression. It could be observed through the small bony gap in the TLS triangle (Fig. 4A). The lower border of the L5 transverse process, the upper border of the sacral ala, and the lateral osteophyte of the S1 superior articular process were drilled out until the lumbosacral ligament was released from the surrounding bony structures. After resection of this ligament, the fifth

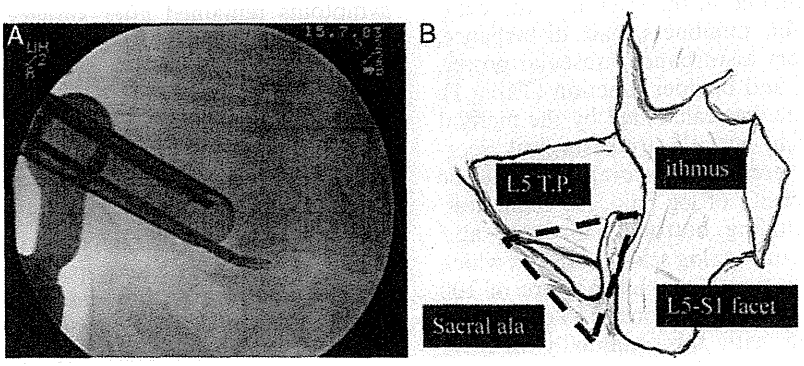

FIGURE 3. Surgical anatomy for spinal microendoscopic extraforaminal decompression. A, Positioning of the tubular retractor is indicated on the photograph taken using an image intensifier. B, The triangle (dotted line) formed by 3 bony structures' configuration (L5 transverse process, lateral aspect of the L5-S1 facet, and the sacral ala; TLS triangle) is the target for nerve decompression.

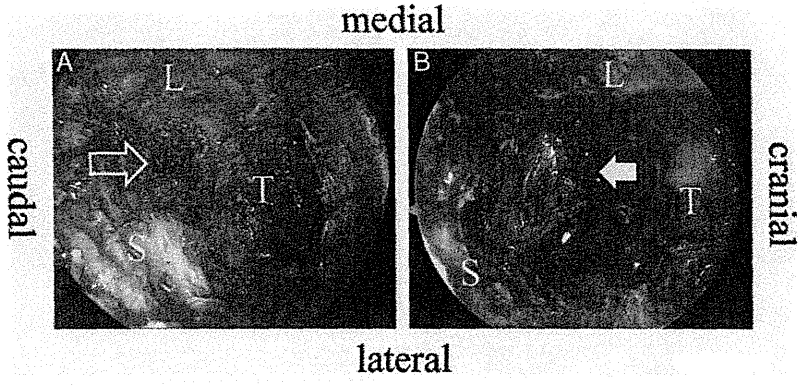

FIGURE 4. Intraoperative spinal microendoscopic views. A, The lower border of the L5 transverse process (T), the lateral aspect of L5-S1 facet (L), and the upper border of the sacral ala (S) are drilled out until the lumbosacral ligament (open white arrow) is released from the surrounding bony structures. B, After resection of the lumbosacral ligament, good decompression of the fifth lumbar spinal nerve is observed (white arrow).

lumbar spinal nerve could be identified (Fig. 4B). This nerve is usually flattened and constricted with thick, dense fibrous tissue. After releasing the constricted fibrous band, further decompression was performed along the nerve laterally and caudally by additional resection of the sacral ala, if necessary. When the nerve was not released completely through this procedure and/or concomitant foraminal stenosis was present, the authors attempted to remove the inferior half part of the pedicle to enlarge the foramen, instead of removing the osteophyte and bulging disc at the L5-S1 segment. Violation of these structures and further resection of facet joint and the pars interarticularis are not recommended because of the risk of inducing lumbar segmental instability after the operation. The patients were allowed to ambulate freely immediately after surgery and were permitted to return to their daily activities without any restrictions.

Clinical Outcome Measures

The surgical outcome was evaluated using the Japanese Orthopaedic Association scoring system (JOA score) for low-back pain before, 6 months after surgery, and at the final follow-up. The assessment items of the JOA scoring system evaluated in the interview and clinical examination are pain, numbness, gait disturbance, straight leg raising, sensory disturbance, muscular power, activities of daily living, and bladder function (Table 1). The average recovery rate was calculated by the method proposed by Hirabayashi et al[16] [(postsurgical score–presurgical score)/(29–presurgical score) × 100] at the final follow-up. The intensity of leg pain, leg numbness, and low-back pain excluding buttock pain were also recorded on a 100 mm visual analog scale (VAS), in which a score of 0 indicates no symptoms and a score of 100 indicates the worst conceivable symptoms. To evaluate the patient's satisfaction with this minimally invasive surgery, the patient was asked to choose 1 of the following responses about the assessment of the surgical treatment according to the criteria adopted from the North American Spine Society Low Back Outcome Instrument[17]: (1) "Surgery met my expectations"; (2) "I did not improve as much as I had hoped, but I would undergo the same surgery for the same outcome"; (3) "Surgery helped, but I would not undergo the same treatment for the same outcome"; or (4) "I am the same as or worse than I was before the surgery." The operation time, estimated blood loss, operative site morbidity, intraoperative and postoperative complications, and need for revision surgery were also recorded.

Statistical Analysis

The data were analyzed using the Wilcoxon signed-rank test for paired groups. The level of significance was set at $P < 0.05$. The results are presented as means ± standard error.

RESULTS

The average age of the patients at the time of surgery was 64.0 ± 11.8 years (range, 41 to 80 y). The mean follow-up period was 37.4 ± 12.1 months (range, 24 to 56 mo) and the mean follow-up rate was 94.1%. Five patients (18.8%) had a history of previous lumbar decompression surgery at the L4-5 segment, and their symptoms remained after surgery. The mean duration between the previous surgery and the index surgery was 39 ± 29 months (range, 3 to 72 mo). All but one patient had not been adequately treated for a long time because their previous back surgery had failed and was diagnosed as failed back surgery syndrome for unknown reasons. The disease duration of other 27 patients was also relatively long. It was 33 ± 36 months (range, 6 to 156 mo). Fifteen of 27 patients had more than 2 years of disease duration. All these patients had failed an initial nonoperative course; however, the treatment option for surgery had not been proposed by previous medical institutes. The main reason for no recommendation of surgery was lack of serious intraspinal canal stenosis in their routine conventional imaging studies.

The disease pathology was spondylosis in 23 patients and degenerative scoliosis in 9 patients. On the

TABLE 1. Scoring System For Low-Back Pain Proposed by Japanese Orthopaedic Association (Maximum 29 Points)

Criteria of the JOA Scoring System	
Items	**Score**
Subjective symptoms (9 points)	
Low-back pain	
None	3
Occasionally mild	2
Always present or sometimes severe	1
Always severe	0
Leg pain and/or numbness	
None	3
Occasionally mild	2
Always present or sometimes severe	1
Always severe	0
Walking ability	3
Normal walking	
Able to walk more than 500 m, pain/numbness/weakness present	2
Unable to walk 500 m due to pain/ numbness/weakness	1
Unable to walk 100 m due to pain/ numbness/weakness	0
Objective findings (6 points)	
Straight leg raising	
Normal	2
30-70 degrees	1
< 30 degrees	0
Sensory function	
Normal	2
Mild sensory disturbance	1
Apparent sensory disturbance	0
Motor function	
Normal (MMT normal)	2
Slight decrease muscle strength (MMT good)	1
Markedly decrease muscle strength (MMT less than fair)	0
Restriction of ADL (14 points)	
None	2
Moderate	1
Severe	0
Bladder function (− 6 points)	
Normal	0
Mild dysuria	− 3
Severe dysuria	− 6
Total score	29

Activities of daily living include the following: turning over while lying down, standing, washing one's face, leaning forward, ability to sit for approximately 1 h, ability to lift or hold heavy objects, and ambulatory ability.

ADL indicates activities of daily living; MMT, manual muscle test.

MR images and myelograms, concomitant intraspinal canal lesions at L4-5 were observed in 14 patients. As there was no method to determine which site was responsible for the clinical symptoms in patients with double lesions, the authors performed simultaneous microendoscopic decompression surgery for each intraspinal canal and extraforaminal lesion. After the operation, all of spine experts in our institute discussed the responsible level together by the video tape and DVD documentation analysis of surgical procedures. When the nerve was free of any impingement and movable without abnormal irritability after surgical exposure alone, we judged the lesion assessed in the preoperative imaging studies as false positive. As per the results, there were no pathologic findings around the nerve roots, such as inflammatory membrane and constriction band in the spinal canal at L4-5, but significant abnormalities were found in the extraforaminal zone at the lumbosacral junction in all patients in this study. In the 18 patients who received the surgery for extraforaminal lesion alone, the mean operation time was 141.6 ± 31.1 minutes, and the mean estimated blood loss was 30.6 ± 38.7 mL. In the 14 patients who received surgery for both intraspinal canal and extraforaminal lesions, the mean operation time was 217.3 ± 35.0 minutes, and the mean estimated blood loss was 37.5 ± 45.6 mL.

No major complications were observed in either group. One patient suffered transient painful dysesthesia immediately after surgery, but this did not progress to neuropathic pain and disappeared after steroid therapy. No patients complained about operative-site morbidity at final follow-up. All patients reported satisfactory pain relief and improvement of neurogenic claudication immediately after surgery, although 4 patients reported later recurrence of their preoperative symptoms. Two of these patients underwent revision surgery 12 months and 33 months after the surgery. The reason for the recurrence of symptoms was residual stenosis in the foramen because of insufficient decompression during the primary surgery.

In the 30 other patients, the mean JOA score was 15.1 ± 4.7 points before surgery, 22.6 ± 3.8 points 6 months after surgery, and 23.1 ± 5.5 points at the final follow-up. The JOA scores improved significantly after surgery ($P < 0.01$), and satisfactory results were maintained until the final follow-up. The mean recovery rate was 60.1% ± 30.5% (Fig. 5). The mean VAS of leg pain decreased significantly from 80.6 ± 17.6 mm preoperatively to 12.4 ± 24.3 mm at the final follow-up ($P < 0.01$). The preoperative VAS of 61.4 ± 32.4 mm for low-back pain also decreased to 29.6 ± 31.3 mm at the final follow-up ($P < 0.01$). The mean VAS of leg numbness improved from 59.7 ± 32.1 to 20.0 ± 26.9 mm ($P < 0.01$) (Fig. 6).

In the patients' self-assessment of the minimally invasive surgery, 18 patients (56.3%) chose "surgery met my expectations" at the follow-up. Ten patients (31.3%) selected "I did not improve as much as I had hoped but I would undergo the same surgery for the same outcome." Of the remaining 4 patients, 2 answered, "surgery helped, but I would not undergo the same treatment for the same outcome" and 2 answered "I am the same as or worse than I was before the surgery (Fig. 7)."

Case Presentations

Case 1

This patient was a 73-year-old woman. This was a surgical failure case. She had undergone the intraspinal canal decompression surgery at the level of L4-5 alone for double lesions of the right fifth lumbar spinal nerve. The primary operations were somewhat effective, but not satisfactory due to postoperative persistent radicular pain and intermittent claudication. The MR image showed no

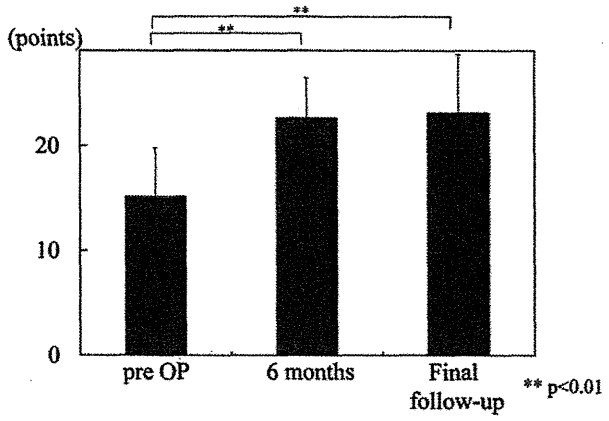

FIGURE 5. Changes in mean Japanese Orthopaedic Association scores before and after surgery. Thirty patients who completed a minimum of 2 years of follow-up after spinal microendoscopic surgery for extraforaminal stenosis at the lumbosacral junction were included in this study. The study group consisted of 16 men and 16 women with an average age at surgery of 64 years and a mean follow-up duration of 37.4 months.

residual stenotic lesion in the spinal canal at the L4-5 segment (Fig. 8A). Local fat reduction was also observed in the extraforaminal zone at the right L5-S1 segment on the axial view (Fig. 8B). As the possibility of a double-crush syndrome was suspected, 3-dimensional-MR imaging study was added to explore the extraforaminal stenosis at the lumbosacral junction. As a result, the fifth lumbar spinal nerve was constricted and swollen at the extraforaminal zone (Fig. 8C). Posterior extraforaminal decompression surgery using a spinal microendoscope was performed to release the impingement of the fifth lumbar spinal nerve between the bony spur of L5 vertebral body and the sacral ala. Immediately after surgery, her leg pain and neurogenic intermittent claudication disappeared completely. 3-dimensional-CT image taken after surgery demonstrated adequate bony decompression without violation of the L5-S1 facet joint (Fig. 8D).

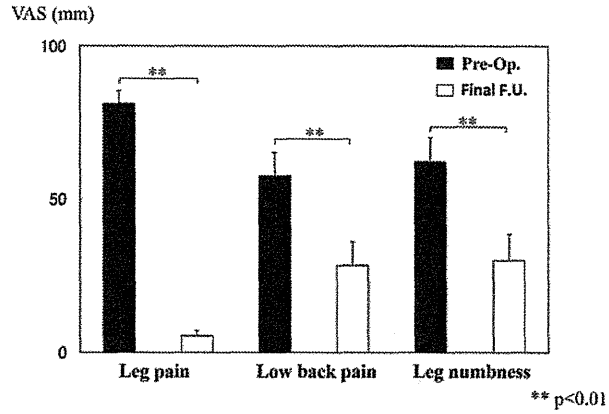

FIGURE 6. Changes in visual analog scale (VAS) before and after surgery. All VAS scores of low back pain, leg pain, and leg numbness had decreased significantly at the final follow-up.

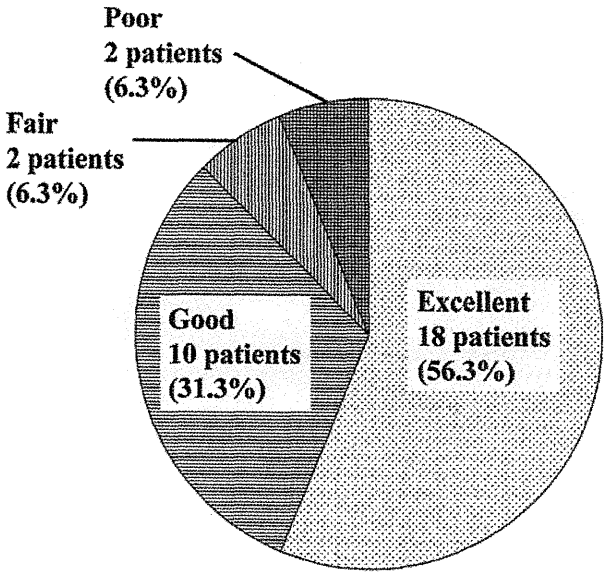

FIGURE 7. The percentage of patient satisfaction. Excellent indicates "Surgery met my expectations." Good indicates "I did not improve as much as I had hoped but I would undergo the same surgery for the same outcome." Fair indicates "Surgery helped, but I would not undergo the same treatment for the same outcome." Poor indicates "I am the same as or worse than I was before the surgery." Almost 90% of the patients treated with spinal microendoscope were satisfied with their surgical results.

DISCUSSION

Spinal microendoscopy allows the surgeon to reach a deep site expeditiously without causing excessive bleeding and muscle damage and provides a bright, magnified visual field. This method seems to have advantages over conventional open methods. The novel minimally invasive surgery also helps to resolve the problem of iatrogenic instability after decompression alone without fusion in cases with extraforaminal stenosis at the lumbosacral junction.[4,18] This is because it can avoid unnecessary invasion of the surrounding tissues other than that required for the nerve decompression procedure.

Various posterior nerve decompression procedures have been used to treat foraminal and/or extraforaminal stenosis at the lumbosacral junction, such as foraminotomy,[4,12] total facetectomy,[1,4,12] osteoplastic hemilaminectomy,[4,19] and lateral fenestration.[4,20–22] These conventional open operative methods often require extensive removal of bone structures to confirm visually that the nerve decompression is sufficient (Fig. 9A). These methods always carry the potential risk of inducing segmental instability, because of violation of the pars interarticularis and facet joint (Fig. 10A). In a clinical case series of patients with foraminal and/or extraforaminal stenosis, Kunogi and Hasue[4] reported that patients with poor clinical results were those who underwent total facetectomy or resection of the pars interarticularis

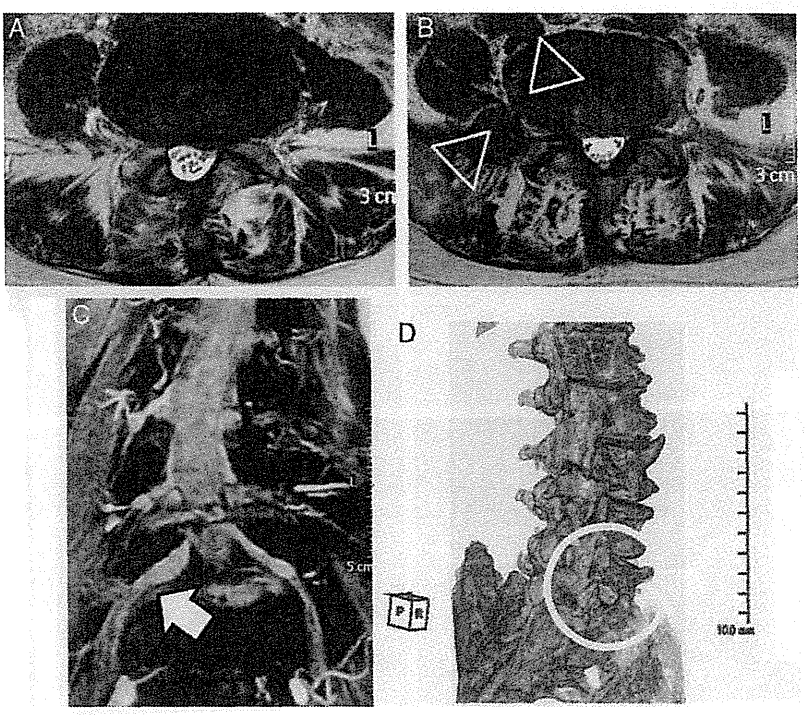

FIGURE 8. Case 1. Images obtained in a 73-year-old woman who presented with severe right leg pain. A, No residual spinal canal stenosis was found at the L4-5 segment. B, The existence of bony stenosis between the bony spur of L5 vertebral body and the sacral ala (white triangle) was suspected. C, On the multiplanar reformat view obtained from 3-dimensional-magnetic resonance imaging studies, extraforaminal entrapment of the fifth lumbar spinal nerve was seen between the sacral ala and osteophyte formation at the L5-S1 segment (white arrow). Swelling of the spinal nerve root and ganglion was also observed. D, 3-dimensional-computed tomography image taken after surgery demonstrated adequate bony decompression without violation of the L5-S1 facet joint.

without fusion. In their opinion, even minimal postoperative spinal instability could adversely affect the nerve root pathologic condition at the foraminal zone. They strongly recommended that spinal fusion after total facetectomy or resection of the pars interarticularis is mandatory, regardless of the patient's age. This recommendation

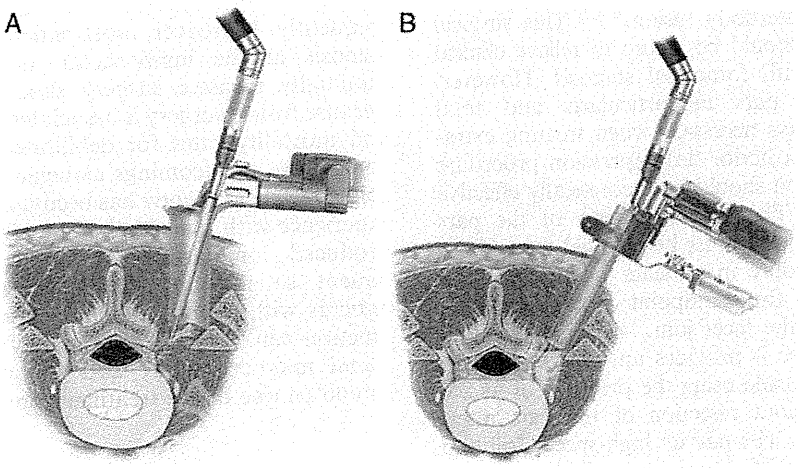

FIGURE 9. Schematic drawings of the comparison of conventional open method and spinal microendoscopic surgery. A, In case of the conventional open surgical method, the facet joint must be sacrificed substantially to place the nerve tissue under direct vision because the operative field is too deep to expose and the back muscle mass and prominence of the posterior iliac crest disturb the visual field and surgical maneuvers. B, Spinal microendoscope can bypass the prominence of the posterior iliac crest. Oblique view from microendoscope provides an illuminated, magnified view of the intraforaminal and extraforaminal zones without unnecessary removal of the facet joint.

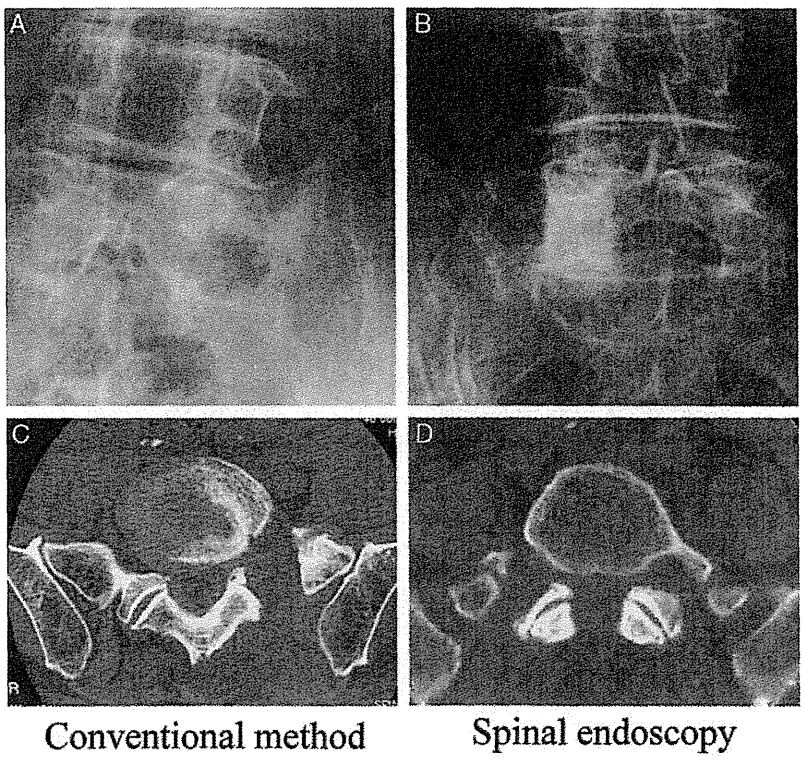

FIGURE 10. Comparison of the configuration of the L5-S1 facet joint on the plain x-rays and computed tomographic scans obtained after surgery. A and C, The nerve decompression procedure resulted in a total facetectomy after the conventional open method. B and D, Spinal microendoscopy could bypass the prominence of the posterior iliac crest and enlarge the foramen with minimal violation of the L5-S1 facet joint.

has led to the tendency to prefer spinal fusion to decompression alone when treating foraminal and/or extraforaminal stenosis.[1,15,18] In particular, there is a recent trend to use an indirect foraminal enlargement procedure and a fusion technique such as posterior lumbar interbody fusion or transforaminal lumbar interbody fusion.[23–25] This surgical strategy is rational and should be secure to relieve clinical symptoms in patients with foraminal stenosis. However, both resection of the pars interarticularis and total facetectomy are not always necessary when treating extraforaminal stenosis. The posterior decompression procedure alone without spinal fusion should be theoretically effective in treating this disease. Therefore, violation of the pars interarticularis and facet joint must be avoided throughout the decompression procedure in patients with only extraforaminal stenosis. From the standpoint of preserving the pars interarticularis and the facet joint, spinal microendoscopy is beneficial because it provides an overview of the intraforamen from the outside using the property of its 25-degree oblique view without resection of the pars interarticularis and facet joint. The curved high-speed drill and Kerrison rongeur developed for spinal microendoscopy are helpful for removing only the osteophyte of the S1 superior facet without the need for facetectomy. This new surgical equipment enables the surgeon to achieve ideal nerve decompression without unnecessary invasion around the intervertebral foramen (Fig. 9B and Fig. 10B).

With respect to fusion surgery, the various biomechanical and clinical studies address cranial segment degeneration.[26–28] Fusion at the L5-S1 segment has a high risk of inducing adjacent segment disc disease at the L4-5 segment where intraspinal canal lesions develop most frequently. Moreover, most patients with extraforaminal stenosis at the lumbosacral junction are older, and minimally invasive surgery should be a high priority because fusion surgery is associated with higher morbidity and mortality rates for debilitated patients.[29] To overcome these shortcomings associated with fusion surgery, spinal microendoscopy has been used in our institute. Our experience with this novel minimally invasive surgery has produced long-lasting favorable outcomes and high patient satisfaction. The authors believe that most patients with extraforaminal stenosis at the lumbosacral junction can be treated effectively without fusion using spinal microendoscope and that this surgical strategy should be one of the treatment options for this disease.

CONCLUSIONS

Spinal microendoscopy is considered a good option for treating extraforaminal stenosis at the lumbosacral junction when the lesion is located deep in the body and is difficult to expose. On account of its oblique view and angled surgical equipments, this method has several

advantages such as providing quick and easy access, avoiding damage to the back muscles, and causing minimal violation of the facet joint and the pars interarticularis. It seems that surgery-induced iatrogenic instability does not occur with this surgical technique. There is a possibility that spinal microendoscopy may replace conventional surgical procedures and become the new standard operating method for treating extraforaminal stenosis at the lumbosacral junction.

REFERENCES

1. Wiltse LL, Guyer RD, Spencer CW, et al. Alar transverse process impingement of the L5 spinal nerve: the far-out syndrome. *Spine.* 1984;9:31–41.
2. Danforth MS, Wilson PD. The anatomy of the lumbosacral region in relation to sciatic pain. *J Bone Joint Surg Am.* 1925;7:109–160.
3. Nathan H, Weizenbluth M, Halperin N. The lumbosacral ligament (LSL) with special emphasis on the "lumbosacral tunnel" and the entrapment of the 5th lumbar nerve. *Int Orthop.* 1982;6:197–202.
4. Kunogi J, Hasue M. Diagnosis, operative treatment of intraforaminal and extraforaminal nerve root compression. *Spine.* 1991; 16:1312–1330.
5. Olsewski JM, Simmons EH, Kallen FC, et al. Evidence from cadavers suggestive of entrapment of fifth lumbar spinal nerves by lumbosacral ligaments. *Spine.* 1991;16:336–347.
6. Transfeldt EE, Robertson D, Bradford DS. Ligaments of the lumbosacral spine and their role in possible extraforaminal spinal nerve entrapment and tethering. *J Spinal Disord.* 1993;6:507–512.
7. Briggs CA, Chandraraj S. Variations in the lumbosacral ligament and associated changes in the lumbosacral region resulting in compression of the fifth dorsal root ganglion and spinal nerve. *Clin Anat.* 1995;8:339–346.
8. Matsumoto M, Chiba K, Nojiri K, et al. Extraforaminal entrapment of the fifth lumbar spinal nerve by osteophytes of the lumbosacral spine: anatomic study and a report of four cases. *Spine.* 2002;27: E169–E173.
9. Matsumoto M, Chiba K, Ishii K, et al. Microendoscopic partial resection of the sacral ala to relieve extraforaminal entrapment of the L-5 spinal nerve at the lumbosacral tunnel: technical note. *J Neurosurg Spine.* 2006;4:342–346.
10. Matsumoto M, Watanabe K, Ishii K, et al. Posterior decompression surgery for extraforaminal entrapment of the fifth lumbar spinal nerve at the lumbosacral junction: clinical article. *J Neurosurg Spine.* 2010;12:72–81.
11. Aota Y, Niwa T, Yoshikawa K, et al. Magnetic resonance imaging and magnetic resonance myelography in the presurgical diagnosis of lumbar foraminal stenosis. *Spine.* 2007;32:896–903.
12. MacNab I. Negative disc exploration: an analysis of the causes of nerve root involvement in sixty-eight patients. *J Bone Joint Surg Am.* 1971;53:891–903.
13. Wiltse LL, Spencer CW. New uses and refinements of the paraspinal approach to the lumbar spine. *Spine.* 1988;13:696–706.
14. Foley KT, Smith MM. Microendoscopic discectomy. *Tech Neurosurg.* 1997;3:301–307.
15. Jenis LG, An HS. Spine update: lumbar foraminal stenosis. *Spine.* 2000;25:389–394.
16. Hirabayashi K, Maruyama T, Wakano K, et al. Postoperative lumbar canal stenosis due to anterior spinal fusion. *Keio J Med.* 1981;30:133–139.
17. Daltroy LH, Cats-Baril WL, Katz JN, et al. The North American Spine Society lumbar spine outcome assessment instrument: reliability and validity tests. *Spine.* 1996;21:741–749.
18. Hambly MF, Wiltse LL, Peek RD, et al. Unilateral lumbar fusion. *Spine.* 1991;16:S295–S297.
19. Kirita Y, Miyazaki K, Hayashi T, et al. Surgical treatment for lumbar disc herniation: osteoplastic partial laminectomy. *Saigai Igaku.* 1975;18:54–62. (In Japanese).
20. Lee CK, Rauschning W, Glenn W. Lateral lumbar spinal canal stenosis: classification, pathologic anatomy and surgical decompression. *Spine.* 1988;13:313–320.
21. Baba H, Uchida K, Maezawa Y, et al. Microsurgical nerve root canal widening without fusion for lumbosacral intervertebral foraminal stenosis: technical notes and early results. *Spinal Cord.* 1996;34:644–650.
22. Reulen HJ, Müller A, Ebeling U. Microsurgical anatomy of the lateral approach to extraforaminal lumbar disc herniations. *Neurosurgery.* 1996;39:345–351.
23. Schlegel J, Champine J, Taylor M, et al. The role of distraction in improving the space available in the lumbar stenotic canal and foramen. *Spine.* 1994;19:2041–2047.
24. Chen D, Fay L, Lok J, et al. Increasing neuroforaminal volume by anterior interbody distraction in degenerative lumbar spine. *Spine.* 1995;20:74–79.
25. Inufusa A, An H, Glover J, et al. The ideal amount of lumbar foraminal distraction for pedicle screw instrumentation. *Spine.* 1996;19:2218–2223.
26. Penta M, Sandu A, Fraser RD. Magnetic resonance imaging assessment of disc degeneration 10 years after anterior lumbar interbody fusion. *Spine.* 1995;20:743–747.
27. Pihlajamaki H, Bostman O, Ruuskanen M, et al. Posterolateral lumbosacral fixation with transpedicular fixation: 63 consecutive cases followed for 4 (2 to 6) years. *Acta Orthop Scand.* 1996;67:63–68.
28. Miyakoshi N, Abe E, Shimada Y, et al. Outcome of one-level posterior lumbar interbody fusion for spondylolisthesis and postoperative intervertebral disc degeneration adjacent to the fusion. *Spine.* 2000;25:1837–1842.
29. Deyo RA, Cherkin DC, Loeser JD, et al. Morbidity and mortality in association with operations on the lumbar spine: the influence of age, diagnosis, and procedure. *J Bone Joint Surg Am.* 1992;74:536–543.

Hindawi Publishing Corporation
Journal of Osteoporosis
Volume 2012, Article ID 642486, 6 pages
doi:10.1155/2012/642486

Research Article

Divergent Significance of Bone Mineral Density Changes in Aging Depending on Sites and Sex Revealed through Separate Analyses of Bone Mineral Content and Area

Yasumoto Matsui,[1] Marie Takemura,[1] Atsushi Harada,[1] Fujiko Ando,[2,3] and Hiroshi Shimokata[3]

[1] *Department of Orthopedic Surgery, National Center for Geriatrics and Gerontology, 35 Gengo, Morioka-cho, Obu 474-8511, Japan*
[2] *Department of Health and Medical Sciences, Aichi Shukutoku University, Nagoya 464-8671, Japan*
[3] *Department for Development of Preventive Medicine, Center for Development of Advanced Medicine for Dementia, National Center for Geriatrics and Gerontology, Obu 474-8511, Japan*

Correspondence should be addressed to Yasumoto Matsui, matsui@ncgg.go.jp

Received 15 June 2012; Revised 27 August 2012; Accepted 24 September 2012

Academic Editor: Harri Sievänen

Bone mineral density (aBMD) is equivalent to bone mineral content (BMC) divided by area. We rechecked the significance of aBMD changes in aging by examining BMC and area separately. Subjects were 1167 community-dwelling Japanese men and women, aged 40–79 years. ABMDs of femoral neck and lumbar spine were assessed by DXA twice, at 6-year intervals. The change rates of BMC and area, as well as aBMD, were calculated and described separately by the age stratum and by sex. In the femoral neck region, aBMDs were significantly decreased in all age strata by an increase in area as well as BMC loss in the same pattern in both sexes. In the lumbar spine region, aBMDs decreased until the age of 60 in women, caused by the significant BMC decrease accompanying the small area change. Very differently in men, aBMDs increased after their 50s due to BMC increase, accompanied by an area increase. Separate analyses of BMC and area change revealed that the significance of aBMD changes in aging was very divergent among sites and between sexes. This may explain in part the dissociation of aBMD change and bone strength, suggesting that we should be more cautious when interpreting the meaning of aBMD change.

1. Introduction

Bone mineral density (aBMD) decreases with age [1] and it is the most significant and widely used index for the diagnosis of osteoporosis and for considering the effects of medication in its treatment [2]. When an aBMD decrease is found, the cause is usually considered to be a decrease in bone mineral content (BMC) in the region measured. ABMD is equivalent to BMC divided by an area. Since areal BMD depends both on bone mineral content and bone dimensions, it is difficult to interpret unambiguously [3]. Dimensional changes occur in long bone by aging [4–6], the shape of the bone, and conditions like osteophytes or vertebral fracture in lumbar spine [7–9] are well known. These can affect the measuring area of DXA examinations, and naturally their results. However, a longitudinal epidemiological DXA study on aging considering the effect of the area has not been carried out on a large scale, although there have been cross-sectional studies [10–17]. This study was performed in order to reconsider the significance of aBMD change and aging in different anatomical locations, by analyzing the longitudinal changes of both components of aBMD, namely, BMC and the area, and comparing the differences in sex. A large cohort for longitudinal studies of local inhabitants was used for this study.

2. Materials and Methods

2.1. Subjects. The subjects were selected among people who participated in both the 1st and 4th waves of the National Institute for Longevity Sciences Longitudinal Study

of Aging (NILS-LSA). Details of the NILS-LSA are presented elsewhere [18]. It is a biannual examination checking the physical and mental condition of ordinary Japanese people, so as to clarify the effect of aging. It is conducted by the National Center for Geriatrics and Gerontology (NCGG), in Japan. The National Institute for Longevity Sciences (NILS) is a research section of NCGG. The participants were chosen randomly from the residents of Obu city and Higashiura-cho, in Aichi prefecture, Japan. For this study, data from 1167 persons were analyzed (59.2 ± 10.9, mean ± SD). Participants were 594 men and 573 women, whose ages ranged from 40 to 79 at the time of the 1st wave. The 1st and 4th waves were from November 1997 to April 2000, and June 2004 to July 2006, respectively.

2.2. Measurements of Bone Mineral Density. Areal bone mineral densities (aBMD) were measured using Hologic QDR4500, both at the 1st and 4th wave. Only one DXA scanner was used. Data on the right femoral neck (Figure 1) and the lumbar spine (L2–4) were used for the analysis. Coefficients of variance of the DXA instrument for aBMD were 1.3% (femoral neck), 1.0% (trochanter), and 0.9% (L2,1–4) [19]. ABMD is equivalent to BMC divided by an area, so the following formula was used for the theoretical calculation: aBMD (g/cm^2) = BMC (g)/Area (cm^2). Therefore, not only aBMD values but also those of BMC and the area measured were used for the analysis in the three different regions above. The annual change rates (CR) were calculated by the following formula. CR (%) = (the values in the 4th−the values in the 1st)/the values in the 1st × 100/6. The CRs of aBMD, BMC, and the area measured were calculated and described separately by the age stratum of 40s, 50s, 60s, and 70s and by sex. All who were 40 to 49 years at baseline belonged to the 40's age stratum, and so forth. Data are presented as the mean ± SD, including those in figures. The study protocol was approved by the Committee on Ethics of Human Research of the National Institute for Longevity Sciences. Written informed consent was obtained from each subject.

2.3. Statistical Analyses. The statistical analyses were made to test for significance of change (versus no change) in each subgroup defined by age decade and sex, using paired t-tests. Also, the trend analyses according to the increase of the age stratum were made for each subgroup using a general linear model procedure. Gender difference was checked for each subgroup. All analyses were conducted using SAS Ver. 8.2 (SAS Institute, Cary, NC, USA).

3. Results

Characteristics of subjects were shown in Table 1.

The change rates (CR) from the first to fourth what were expressed as an annual rate. Mean variation between the two DXA measurements was 6 years.

3.1. Femoral Neck Region. ABMDs significantly decreased in all age strata both in women (−1.1 ± 1.1% in 40s, −1.2 ± 0.9% in 50s, −1.0 ± 0.9% in 60s, and −0.8 ± 1.1% in 70s, all $P < 0.01$) and in men (−0.4 ± 0.8% in 40s, −0.5 ± 0.7% in 50s, −0.6 ± 0.9% in 60s, and −0.6 ± 1.0% in 70s, all $P < 0.01$) (Figures 2(a) and 2(b)). These declines were caused not merely by the decrease of BMC in most of the age strata (in women, −0.7 ± 1.4% in 40s, −0.8 ± 1.2% in 50s, and −0.4 ± 1.2% in 60s, all $P < 0.01$, and in men, −0.2 ± 0.9% in 50s and −0.2 ± 1.1% in 70s, with $P < 0.01$ and $P < 0.05$, resp.), but also by the constant or significant increase of the area measured (in women, 0.4 ± 1.1% in 40s, 0.5 ± 1.1% in 50s, 0.6 ± 1.2% in 60s, and 0.5 ± 1.5% in 70s, all $P < 0.01$, and in men, 0.4 ± 0.6% in 40s, 0.3 ± 0.8% in 50s, 0.4 ± 0.8% in 60s, and in 0.4 ± 0.8% in 70s, all $P < 0.01$). This trend was the same in both sexes. The change rates (CR) of the aBMD and BMC, however, were different between women and men in their 40s, 50s, and 60s (Table 2). The CR became higher (in absolute value) only in women according to age in aBMD and BMC (P trend = 0.0126 and 0.0027, resp.). As for the CR of the area, no significant trend according to age was observed in both sexes, and no sex difference was observed (Table 2).

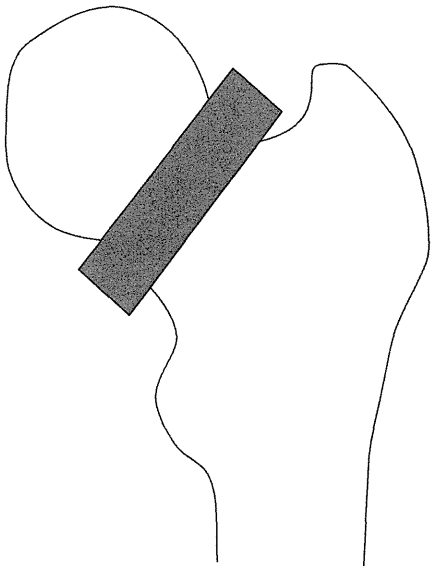

FIGURE 1: Femoral neck region of interest, derived from the Hologic QDR 4500 Operator's Manual.

3.2. Lumbar Spine Region. ABMDs significantly decreased in women in their 40s, 50s, and 60s (−1.1 ± 1.2% in 40s, −1.0 ± 0.9% in 50s, and −0.2 ± 1.1 in 60s, with $P < 0.01$, $P < 0.01$ and $P < 0.05$, resp.) (Figure 3(a)). At earlier ages, these declines were caused by a significant decrease in BMC (−1.2 ± 1.5% in 40s and −1.2 ± 1.2% in 50s, both $P < 0.01$) accompanied by a small but significant decrease in the area. After their 60s, however, no further decrease in BMC occurred, and the small but significant increase of aBMD was caused by the significant increase in the area.

The patterns of aBMD changes were much different in men. BMDs significantly increased in the 50s, 60s, and 70s (0.3 ± 0.8%, 0.5 ± 1.5%, and 0.3 ± 1.0%, all $P < 0.01$) due to

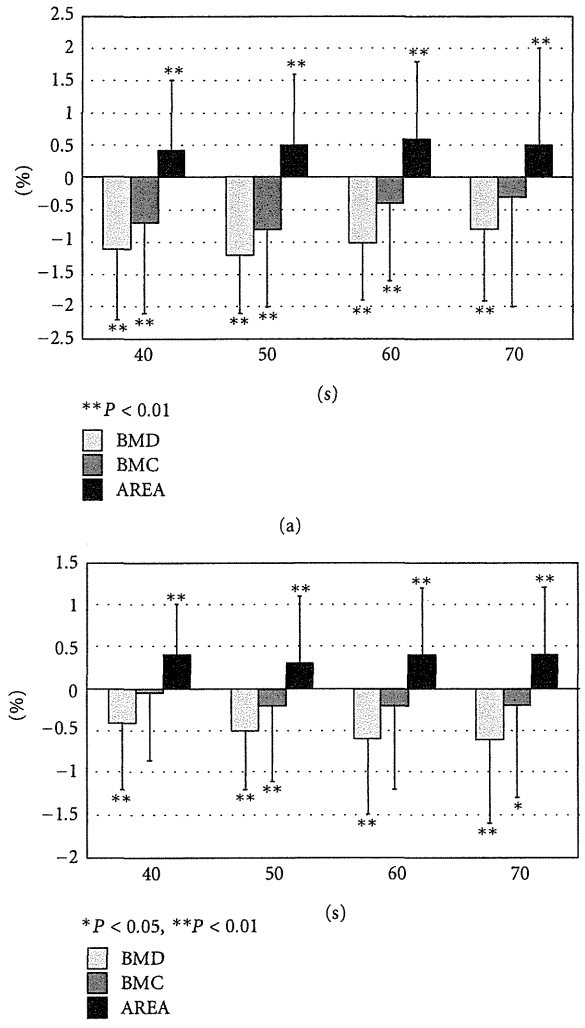

FIGURE 2: (a) Changes in the femoral neck region by age group in women. Results are the mean (±SD) CR of four different age strata. $^{**}P < 0.01$. (b) Changes in the femoral neck region by age group in men. Results are the mean (±SD) CR of four different age strata. $^{*}P < 0.05$, $^{**}P < 0.01$.

the significant increase of BMC (0.5 ± 1.0% in 50s, 1.0 ± 3.4% in 60s, and 0.4 ± 1.2% in 70s, all $P < 0.01$) (Figure 3(b)). The areas significantly increased in every age stratum (0.1 ± 0.5% in 40s, 0.2 ± 0.5% in 50s, 0.4 ± 1.2% in 60s, and 0.2 ± 0.6% in 70s, all $P < 0.01$). Since the increase of BMD occurred after the 50s, the rates of BMC increase surpassed those of the area. The change rates (CR) of the aBMD, BMC, and area were different between women and men in their 40s, 50s, and 60s (Table 2). And in women the CR increased according to age in aBMD, BMC, and area (P trend <0 .0001, P trend <0.0001, and P trend = 0.0115, resp.). The CR increased in men according to age in aBMD and BMC (P trend= 0.006 and P trend = 0.027, resp.), but not in area (Table 2).

TABLE 1: Characteristics of subjects.

	Women	Men
Age (years)	56.5 ± 9.9	57.9 ± 9.9
Height (cm)		
All	152.2 ± 5.7 (n = 573)	165.4 ± 5.9 (n = 594)
40s	154.9 ± 5.0 (n = 168)	168.7 ± 5.5 (n = 148)
50s	153.3 ± 4.8 (n = 179)	166.3 ± 5.7 (n = 183)
60s	150.4 ± 5.6 (n = 147)	164.0 ± 4.7 (n = 162)
70s	147.0 ± 5.0 (n = 79)	161.0 ± 5.2 (n = 101)
Weight (kg)		
All	53.0 ± 8.0 (n = 573)	62.8 ± 8.5 (n = 594)
40s	54.1 ± 8.0 (n = 168)	66.4 ± 8.8 (n = 148)
50s	53.7 ± 7.4 (n = 179)	63.5 ± 8.1 (n = 183)
60s	53.0 ± 8.0 (n = 147)	61.2 ± 7.8 (n = 162)
70s	49.1 ± 7.9 (n = 79)	58.8 ± 7.5 (n = 101)
BMI (kg/m^2)		
All	22.9 ± 3.2 (n = 573)	22.9 ± 2.6 (n = 594)
40s	22.5 ± 3.3 (n = 168)	23.3 ± 2.6 (n = 148)
50s	22.9 ± 3.2 (n = 179)	23.0 ± 2.5 (n = 183)
60s	23.4 ± 3.1 (n = 147)	22.8 ± 2.7 (n = 162)
70s	22.7 ± 3.1 (n = 79)	22.6 ± 2.5 (n = 101)
BMD at 1st wave		
Femoral neck (g/cm^2)	0.7 ± 0.1	0.8 ± 0.1
Trochanter (g/cm^2)	0.6 ± 0.1	0.7 ± 0.1
Lumbar spine (L2–4) (g/cm^2)	0.9 ± 0.2	1.0 ± 0.2
BMC at 1st wave		
Femoral neck (g)	3.2 ± 0.6	4.0 ± 0.7
Trochanter (g)	6.0 ± 1.3	8.7 ± 1.6
Lumbar spine (L2–4) (g)	38.1 ± 9.3	50.7 ± 10.0
Area at 1st wave		
Femoral neck (cm^2)	4.6 ± 0.3	5.3 ± 0.3
Trochanter (cm^2)	10.2 ± 1.2	12.8 ± 1.4
Lumbar spine (L2–4) (cm^2)	42.3 ± 3.9	51.3 ± 4.5

Values are mean ± SD.

4. Discussion

ABMD is equivalent to BMC divided by an area, but when we encounter cases of BMD decline, we simply consider the decline of the BMC at the measured sites without

TABLE 2: P trend according to age strata and P value of sex difference analyses of subgroup.

		P trend according to age strata		Sex difference analysis			
		women	men	40s	50s	60s	70s
Femoral neck	BMD	0.0126	0.1682	<0.0001	<0.0001	<0.0001	0.0982
	BMC	0.0027	0.2519	<0.0001	<0.0001	0.0298	0.7122
	Area	0.2084	0.9947	0.9436	0.0434	0.0987	0.2391
Lumbar spine	BMD	<0.0001	0.006	<0.0001	<0.0001	<0.0001	0.815
	BMC	<0.0001	0.027	<0.0001	<0.0001	<0.0001	0.4277
	Area	0.0115	0.3383	<0.0001	<0.0001	0.0052	0.0986

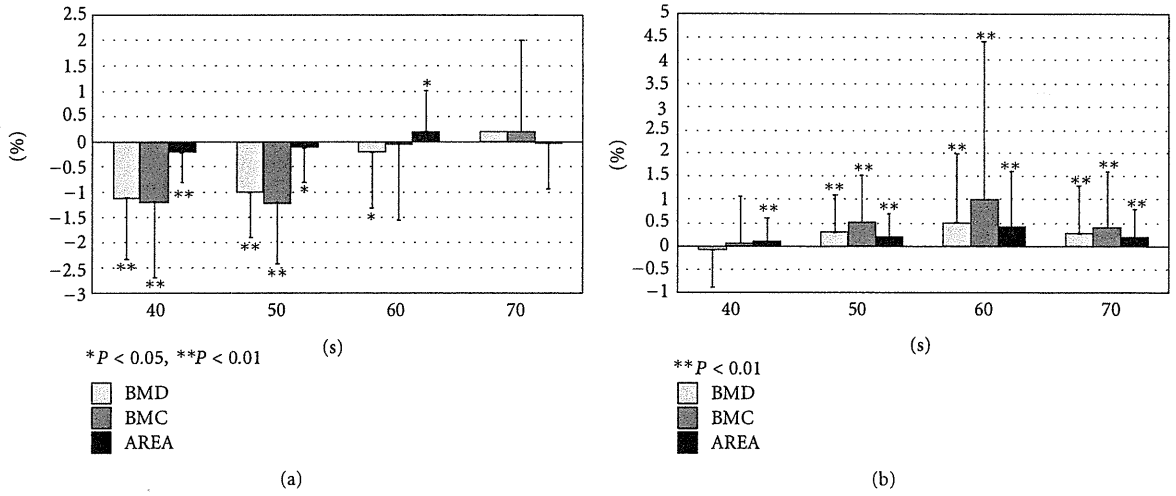

FIGURE 3: (a) Changes in the lumbar spine region by age group in women. Results are the mean (±SD) CR of four different age strata. *$P < 0.05$, **$P < 0.01$. (b) Changes in the lumbar spine region by age group in men. Results are the mean (±SD) CR of four different age strata. **$P < 0.01$.

incorporating the change of the area (or size), which may represent the change of the shape in the region. The present study demonstrated that in the femoral neck, the aBMD decline in aging occurs not only due to the decline of BMC, but also due to the increase in the area, for both men and women. In fact, the increase of the femoral neck area represents the physiological compensating effect of the weakened bone tolerance [4, 20–23], caused by BMC decline. This may be one of the reasons for the dissociation between the strength of the bone and aBMD values. The widening (or enlargement) of the femoral neck in elderly persons has been demonstrated by the hip structure analyses of DXA [10, 13–15], by computed tomography [23–26], or utilizing both [27, 28]. The annual change rates of aBMD in our study in the femoral neck region were around −1% in women (Figure 2(a)) and 0.5% in men (Figure 2(b)). This is almost equal to the level of the large population-based cohort in Hiroshima Japan, −1.14% in women, and −0.38% in men [29]. In the lumbar spine, however, a sexual difference was observed in the changes of aBMD and those of BMC or the area as well. The increase in BMC together with the area may be explained by the osteophyte formation found to be more marked in elderly men [7, 9]. This type of change, osteophyte formation, occurs also in women but later. The significant area increase in women may derive from the osteophyte formation in advanced age. The reason for the significant decrease in the areas in women in their 40s and 50s is unclear at the moment. More detailed studies, using CT scans, are warranted to elucidate the mechanism of the sex difference in the spinal region.

From this perspective, the meaning or significance of aBMD change should be diverse depending on the sites measured and gender. Moreover, the apparent decrease of aBMD may not simply represent the weakness of that measured region (e.g., in the femoral neck), since the greater diameter can make the cylindrical structure stronger [21].

The limitation of this study is that the measurements were carried out by the ordinary DXA method without using elaborate software like hip structure analysis or CT. DXA has an inherent inaccuracy [30–32]. If body composition or weight changed during the followup, it is possible that BMD is inaccurately measured, namely, it may be over- or underestimated. Also, the size measuring by DXA was not very accurate for volumetric analysis. But our method disclosed the differences among sites and between sexes, particularly in terms of longitudinal effect, which have been little investigated.

The strength of our study is its random selection of our samples from people in the local community with very little bias in the process. NILS-LSA is one of the few major epidemiological studies investigating the aging mechanism that is designed to select subjects in a completely random manner. The results of this study should therefore reveal characteristics of the entire Japanese population.

In summary, we investigated the meaning of aBMD changes in aging through separate analyses of BMC and area change. The results revealed that the significance of aBMD changes were very divergent among the sites measured, and between sexes. This may explain the dissociation of aBMD change and bone strength, which encourages one to be more cautious when interpreting the meaning of aBMD change.

Acknowledgment

This work was supported by the research fund for Longevity Sciences [23–33] from the National Center for Geriatrics and Gerontology (NCGG), Japan.

References

[1] P. Steiger, S. R. Cummings, D. M. Black, N. E. Spencer, and H. K. Genant, "Age-related decrements in bone mineral density in women over 65," *Journal of Bone and Mineral Research*, vol. 7, no. 6, pp. 625–632, 1992.

[2] S. R. Cummings, D. Bates, and D. M. Black, "Clinical use of bone densitometry: scientific review," *Journal of the American Medical Association*, vol. 288, no. 15, pp. 1889–1897, 2002.

[3] H. Sievänen, "A physical model for dual-energy X-ray absorptiometry-derived bone mineral density," *Investigative Radiology*, vol. 35, no. 5, pp. 325–330, 2000.

[4] C. B. Ruff and W. C. Hayes, "Subperiosteal expansion and cortical remodeling of the human femur and tibia with aging," *Science*, vol. 217, no. 4563, pp. 945–948, 1982.

[5] R. P. Heaney, M. J. Barger-Lux, K. M. Davies, R. A. Ryan, M. L. Johnson, and G. Gong, "Bone dimensional change with age: interactions of genetic, hormonal, and body size variables," *Osteoporosis International*, vol. 7, no. 5, pp. 426–431, 1997.

[6] H. G. Ahlborg, O. Johnell, C. H. Turner, G. Rannevik, and M. K. Karlsson, "Bone loss and bone size after menopause," *New England Journal of Medicine*, vol. 349, no. 4, pp. 327–334, 2003.

[7] H. Kinoshita, T. Tamaki, T. Hashimoto, and F. Kasagi, "Factors influencing lumbar spine bone mineral density assessment by dual-energy X-ray absorptiometry: comparison with lumbar spinal radiogram," *Journal of Orthopaedic Science*, vol. 3, no. 1, pp. 3–9, 1998.

[8] A. Atalay, M. Kozakcioglu, R. Cubuk, N. Tasali, and S. Guney, "Degeneration of the lumbar spine and dual-energy X-ray absorptiometry measurements in patients without osteoporosis," *Clinical Imaging*, vol. 33, no. 5, pp. 374–378, 2009.

[9] Ö Karabulut, M. C. Tuncer, Z. Karabulut, A. Açlkgöz, E. S. Hatipoğlu, and Z. Akkuş, "Relationship between radiographic features and bone mineral density in elderly men," *Folia Morphologica*, vol. 69, no. 3, pp. 170–176, 2010.

[10] T. J. Beck, C. B. Ruff, W. W. Scott Jr., C. C. Plato, J. D. Tobin, and C. A. Quan, "Sex differences in geometry of the femoral neck with aging: a structural analysis of bone mineral data," *Calcified Tissue International*, vol. 50, no. 1, pp. 24–29, 1992.

[11] K. S. Tsai, W. C. Cheng, C. K. Chen et al., "Effect of bone area on spine density in Chinese men and women in Taiwan," *Bone*, vol. 21, no. 6, pp. 547–551, 1997.

[12] M. Peacock, G. Liu, M. Carey et al., "Bone mass and structure at the hip in men and women over the age of 60 years," *Osteoporosis International*, vol. 8, no. 3, pp. 231–239, 1998.

[13] T. J. Beck, A. C. Looker, C. B. Ruff, H. Sievanen, and H. W. Wahner, "Structural trends in the aging femoral neck and proximal shaft: analysis of the Third National Health and Nutrition Examination Survey dual-energy x-ray absorptiometry data," *Journal of Bone and Mineral Research*, vol. 15, no. 12, pp. 2297–2304, 2000.

[14] S. Kaptoge, N. Dalzell, N. Loveridge, T. J. Beck, K. T. Khaw, and J. Reeve, "Effects of gender, anthropometric variables, and aging on the evolution of hip strength in men and women aged over 65," *Bone*, vol. 32, no. 5, pp. 561–570, 2003.

[15] D. A. Nelson, J. M. Pettifor, D. A. Barondess, D. D. Cody, K. Uusi-Rasi, and T. J. Beck, "Comparison of cross-sectional geometry of the proximal femur in white and black women from Detroit and Johannesburg," *Journal of Bone and Mineral Research*, vol. 19, no. 4, pp. 560–565, 2004.

[16] X. F. Wang, Y. Duan, T. J. Beck, and E. Seeman, "Varying contributions of growth and ageing to racial and sex differences in femoral neck structure and strength in old age," *Bone*, vol. 36, no. 6, pp. 978–986, 2005.

[17] A. C. Looker, H. W. Wahner, W. L. Dunn et al., "Updated data on proximal femur bone mineral levels of US adults," *Osteoporosis International*, vol. 8, no. 5, pp. 468–489, 1998.

[18] H. Shimokata, F. Ando, and N. Niino, "A new comprehensive study on aging—the National Institute for Longevity Sciences, Longitudinal Study of Aging (NILS-LSA)," *Journal of Epidemiology*, vol. 10, no. 1, pp. S1–S9, 2000.

[19] Y. Yamada, F. Ando, N. Niino, and H. Shimokata, "Association of polymorphisms of interleukin-6, osteocalcin, and vitamin D receptor genes, alone or in combination, with bone mineral density in community-dwelling Japanese women and men," *Journal of Clinical Endocrinology and Metabolism*, vol. 88, no. 7, pp. 3372–3378, 2003.

[20] B. Martin, "Aging and strength of bone as a structural material," *Calcified Tissue International*, vol. 53, supplement 1, pp. S34–S39, 1993.

[21] E. Seeman, "Periosteal bone formation—a neglected determinant of bone strength," *New England Journal of Medicine*, vol. 349, no. 4, pp. 320–323, 2003.

[22] E. S. Orwoll, "Toward an expanded understanding of the role of the periosteum in skeletal health," *Journal of Bone and Mineral Research*, vol. 18, no. 6, pp. 949–954, 2003.

[23] C. R. Russo, F. Lauretani, E. Seeman et al., "Structural adaptations to bone loss in aging men and women," *Bone*, vol. 38, no. 1, pp. 112–118, 2006.

[24] T. F. Lang, J. H. Keyak, M. W. Heitz et al., "Volumetric quantitative computed tomography of the proximal femur: precision and relation to bone strength," *Bone*, vol. 21, no. 1, pp. 101–108, 1997.

[25] B. L. Riggs, L. J. Melton III, R. A. Robb et al., "Population-based study of age and sex differences in bone volumetric density, size, geometry, and structure at different skeletal sites," *Journal of Bone and Mineral Research*, vol. 19, no. 12, pp. 1945–1954, 2004.

[26] L. M. Marshall, T. F. Lang, L. C. Lambert, J. M. Zmuda, K. E. Ensrud, and E. S. Orwoll, "Dimensions and volumetric BMD of the proximal femur and their relation to age among older U.S. men," *Journal of Bone and Mineral Research*, vol. 21, no. 8, pp. 1197–1206, 2006.

[27] J. S. Bauer, S. Kohlmann, F. Eckstein, D. Mueller, E. M. Lochmüller, and T. M. Link, "Structural analysis of trabecular bone of the proximal femur using multislice computed tomography: a comparison with dual X-ray absorptiometry for predicting biomechanical strength in vitro," *Calcified Tissue International*, vol. 78, no. 2, pp. 78–89, 2006.

[28] L. M. Havill, M. C. Mahaney, T. L. Binkley, and B. L. Specker, "Effects of genes, sex, age, and activity on BMC, bone size, and areal and volumetric BMD," *Journal of Bone and Mineral Research*, vol. 22, no. 5, pp. 737–746, 2007.

[29] N. Masunari, S. Fujiwara, Y. Nakata, K. Furukawa, and F. Kasagi, "Effect of angiotensin converting enzyme inhibitor and benzodiazepine intake on bone loss in older Japanese," *Hiroshima Journal of Medical Sciences*, vol. 57, no. 1, pp. 17–25, 2008.

[30] J. M. P. Soriano, E. Ioannidou, J. Wang et al., "Pencil-beam versus fan-beam dual-energy X-ray absorptiometry comparisons across four systems: body composition and bone mineral," *Journal of Clinical Densitometry*, vol. 7, no. 3, pp. 281–289, 2004.

[31] H. H. Bolotin and H. Sievänen, "Inaccuracies inherent in dual-energy x-ray absorptiometry in vivo bone mineral density can seriously mislead diagnostic/prognostic interpretations of patient-specific bone fragility," *Journal of Bone and Mineral Research*, vol. 16, no. 5, pp. 799–805, 2001.

[32] H. H. Bolotin, H. Sievänen, J. L. Grashuis, J. W. Kuiper, and T. L. N. Järvinen, "Inaccuracies inherent in patient-specific dual-energy X-ray absorptiometry bone mineral density measurements: Comprehensive phantom-based evaluation," *Journal of Bone and Mineral Research*, vol. 16, no. 2, pp. 417–426, 2001.

[33] H. H. Bolotin, H. Sievänen, and J. L. Grashuis, "Patient-specific DXA bone mineral density inaccuracies: quantitative effects of nonuniform extraosseous fat distributions," *Journal of Bone and Mineral Research*, vol. 18, no. 6, pp. 1020–1027, 2003.